Grafting of lanthanide complexes on silica surfaces dehydroxylated at 200 °C: a theoretical investigation

Iker Del rosal, I.C. Gerber, Romuald Poteau, Laurent Maron

NJC

Accepted Manuscript

This is an *Accepted Manuscript*, which has been through the Royal Society of Chemistry peer review process and has been accepted for publication.

Accepted Manuscripts are published online shortly after acceptance, before technical editing, formatting and proof reading. Using this free service, authors can make their results available to the community, in citable form, before we publish the edited article. We will replace this *Accepted Manuscript* with the edited and formatted *Advance Article* as soon as it is available.

You can find more information about *Accepted Manuscripts* in the Information for Authors.

Please note that technical editing may introduce minor changes to the text and/or graphics, which may alter content. The journal's standard Terms & Conditions and the Ethical guidelines still apply. In no event shall the Royal Society of Chemistry be held responsible for any errors or omissions in this *Accepted Manuscript* or any consequences arising from the use of any information it contains.

ROYAL SOCIETY OF CHEMISTRY

www.rsc.org/njc

Grafting of lanthanide complexes on silica surfaces dehydroxylated at 200°C : A theoretical investigation

Del Rosal Iker, Gerber Iann C., Poteau Romuald, Maron Laurent*

1. Université de Toulouse ; INSA, UPS ; LPCNO (IRSAMC) ; 135 avenue de Rangueil, F-31077 Toulouse, France

2. CNRS ; UMR 5215 (IRSAMC) ; F-31077 Toulouse, France

e-mail: laurent.maron@irsamc.ups-tlse.fr

Abstract

Cluster models of SiO_2-200 are proposed and compared with spectroscopic (IR and NMR) experimental data. Five models describing the variety of surface silanols (isolated, vicinal and germinal) at the SiO_2-200 surface have then been derived and used to study the grafting reaction of homoleptic silylamide lanthanum(III) complexes. Three different grafting modes have been obtained (mono-, bi- and tri-grafted) in line with the experimental knowledge. In terms of energetic stability as well as spectroscopic properties of coordinated OPPh3 (as a probe), all modes could coexist at the surface. The analysis of the $\delta(^{31}P)$ chemical shifts for the coordinated OPPh3 indicates some possible important differences in Lewis acidity of the lanthanide centre, that may impact the catalysis.

1 Introduction

In the context of the research of low cost and environmentally benign catalytic systems[1], developments of highly active and selective catalysts are of prime importance. From an industrial point of view, heterogeneous processes are advantageous because of the facile separation of the final products from the catalysts, and the easy recycling of these catalysts which results in lower operating cost. Moreover, the easier solid-liquid separation reduces the solvent consumption which is in agreement with the constant demand for greener chemical processes. In the case of homogeneous catalysts, every entity can act as a single active site. This makes homogeneous catalysts intrinsically more active and selective compared to heterogeneous catalysts. Therefore, a catalytic system, which takes the advantages of both homogeneous and heterogeneous catalysis, would greatly enhance the interest for industrial applications. One possibility to achieve this type of catalytic system is the use of supported catalysts (or the heterogenization of homogeneous catalysts). In this way, silica surface is an attractive candidate to be used as catalyst support. The use of SiO_2 is principally due to the large surface area, the good mechanical and thermal properties of this oxide but also because SiO_2 does not generate parallel reactions. Moreover, silica is a highly versatile material since one can choose between e.g. crystalline, mesoporous and amorphous silica as well as different thermal treatment of the surface (ranging from 200°C to 750°C). The former would change the specific area of the surface whereas the latter would lead to a difference of surface silanols inducing a diversity of grafted complexes at the surface. In all cases, there is a reasonable knowledge of its surface structure in order to understand its reactivity with metal complexes[2.] The use of silica for the grafting of catalytically active metal complexes or for hosting metal particles at the surface makes that silica is considered an excellent material in catalysis[3].

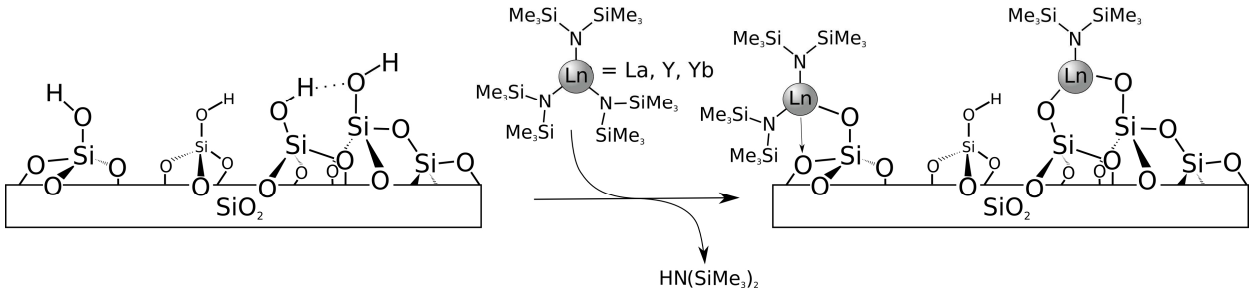

Figure 1. Schematic representation of the possible surface species obtained by the grafting reaction of lanthanide silylamides on a dehydroxylated silica surface at 250°C [4a,b].

Among the metals applied within the field of catalysis, rare-earth systems have been the subject of constant interest, due to their high activity in several fields, such as in polymerization[4] and fine chemistry[5], their low toxicity and their moderate cost. However, among the large variety of reported lanthanide complexes, amido derivatives have been found to be one of the most attractive and

versatile family. The experimental grafting reaction of homoleptic derivatives, of the type $Ln(N(SiMe_3)_2)_3$ [Ln= Y, La, Nd, Sm], have already been described by Anwander et al.[6] among others[4,7] (see Figure 1). As shown by Anwander et al. in 1997, these compounds react with silica's hydroxyl groups, leading to the formation of a covalent lanthanide-siloxide bond with the concomitant protonolysis of the lanthanide-amido bond[6,8]. The experimental elemental analysis of this grafting reaction[4] shows that the metal content is similar for materials prepared from the same support, i.e., after the same heat pre-treatments. Thus, this analysis indicates that the grafting reaction proceeds with similar efficiency for yttrium, lanthanum, neodymium and samarium species. In the same way, the elemental analysis reveals that the N – La molar monografted:bigrafted ratio increases with the pre-treatment temperature, from 25:75 at 250°C to 55:45 at 500°C and 100:0 at 700°C. Since then, several grafted species based on these metals were synthesized. The bare[9] and grafted[4b,10] silica surfaces have been characterized by thermogravimetry, IR and NMR spectroscopy. Some of the catalytic properties of grafted complexes were also studied by considering different reactions such as the Danishefsky reaction[5a,b], the alkynes dimerization or the alkenes hydrosilylation[5c], the intramolecular Hydroamination/Cyclization of Aminoalkenes[5d] and the ethylene, ε-caprolactone and isoprene polymerization reaction[4]. However, it should be noticed that experimental data do not give enough information to determine the grafting mode of the lanthanide complex. In a previous work[11], we created realistic molecular models for a silica surface partially dehydroxylated at 700°C ($SiO_{2\text{-}700}$). After a first selection based on the rigidity of the ligand, the surface density of silanol groups, and IR frequencies of the hydroxyl groups of the silanols, two possible models of the surface have henceforth been considered, in agreement with a similar work realized considering a periodic supercell model[12]. The thermodynamics of a grafting reaction of lanthanum catalysts on these models has also been investigated. This reaction leads to thermodynamically stable structures that reveal different grafting modes: mono-grafted, bi-grafted or bi-grafted after breaking of a Si-O-Si bridge. This study highlights that the grafting in a top position is not favorable, and there are two relevant grafting modes when the coordination site is an isolated silanol: on one hand a mono-grafted complex in a bridging position (scheme 1a), and on the other hand a bi-grafted catalyst by the break of a siloxane bridge (scheme 1b).

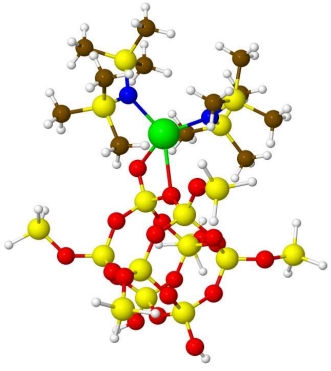

a

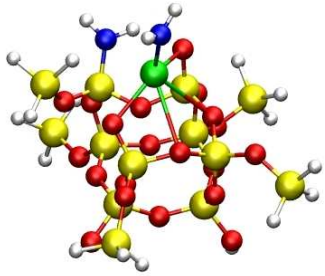

b

Scheme 1 : Favorable grafting modes on isolated silanol. a (left) the monografted bridging mode and b (right) the bigrafted mode with a broken Si-O-Si bridge

Surface organometallic chemistry on $SiO_{2\text{-}200}$ is less straightforward than that of $SiO_{2\text{-}700}$, as expected from the several types of silanol groups present on its surface, leading to a possible coexistence of several grafting modes at the SiO_2 surface. Indeed, during the dehydroxylation process the silanol groups are condensed in pairs, producing one water molecule and one siloxane bond. The condensation of surface silanols at 700°C induces the formation of isolated silanol groups (≡ SiOH, Q^3), where the surface silicon atom has three bonds into the bulk structure and the fourth to one OH group (see Figure 2). These silanol groups are considered isolated when they cannot be involved in a hydrogen bond interaction. When the silica surface is treated at 200°C, we can observe the presence of isolated silanol groups but also geminal silanols (= $Si(OH)_2$, Q^2) when two hydroxyl groups are attached to the same silicon atom and vicinal silanols (Q^3) when an isolated silanol groups is connected by an oxygen atom or hydrogen bonded to another silanol group.

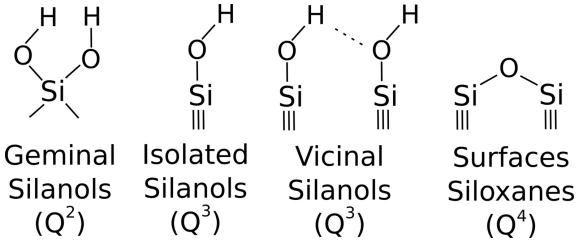

Figure 2. Q^n nomenclature used to define the environment of the silicon atoms in silica

We report here results on the grafting of lanthanide silylamide complexes onto a dehydroxylated silica at 200°C where, with respect to a silica pre-treated at 700°C, other grafting modes might be available due to the higher density of silanol groups at the surface. This study will be divided into two parts. The first part is devoted to the validation of the created surface cluster models of a silica surface partially dehydroxylated at 200°C, compatible with different structural and spectroscopic experimental data. Indeed, the modeling of amorphous supports is still a challenge for computational chemists because of the complexity of amorphous systems which would require expensive calculations. In general, two strategies have been adopted to compute the electronic structure of silica and its defects: the cluster approach[13] and the periodic boundary conditions approach[14]. In general, the computational modeling of amorphous solids using periodic boundary conditions is usually considered as the most relevant approach because it takes into account the extended nature of the material. Nevertheless, a study carried out by Solans-Monfort et al.[15] has shown that the experimental characteristic data are well reproduced and nearly identical for cluster models and periodic systems. In this study, we have chosen the cage-like cluster approach to model

the silicate surface, which allows easier investigations of multi-step reactions mechanisms. The second part of our study involves another important step of the surface organometallic chemistry, which is the interaction between lanthanide catalysts and the SiO_{2-200} surface. Experimental works, involving IR and NMR spectroscopy, were carried out to determine the nature of the grafting mode on the surface and among others, the coordination of Triphenylphosphine Oxide ($O=PPh_3$) was reported by Gauvin et al.[5c]. Therefore, based on these experimental reports, different coordination modes of $Ln(N(SiMe_3)_2)_3@SiO_{2-200}$ have been computed, spectroscopically characterized and compared with experiments. The knowledge of the catalyst grafting mode is crucial because it conditions all the parameters of reaction pathways: kinetic and thermodynamic data, regioselectivity and stereoselectivity.

2 Computational Details

All DFT calculations were performed with Gaussian 03[16]. Calculations were carried out at the DFT level of theory using the hybrid functional B3PW91[17]. Geometry optimizations were achieved without any symmetry restriction. Calculations of vibrational frequencies were systematically done in order to characterize the nature of stationary points. Stuttgart effective core potentials[18] and their associated basis set were used for silicon, yttrium, lanthanum, neodymium and ytterbium . The basis sets were augmented by a set of polarization functions (ζ_d = 0.284 for Si and ζ_f = 1.000 for Y, La, Nd and Yb). Hydrogen, nitrogen and oxygen atoms were treated with 6-31G(d, p) double- ζ basis sets[19]. Among the various theories available to compute chemical shielding tensors, the gauge including atomic orbital (GIAO) method has been adopted for the numerous advantages it presents[20]. The same methodology was used in previous work involving grafted systems showing that theoretical results are fairly accurate with respect to experimental values with an error lower than 15% for ^{29}Si [11], 10% for ^{31}P [21a] and ^{17}O[21b,c,d] and 5% for ^{1}H [21e] and ^{13}C [21e]. The electron density and partial charge distribution were examined in terms of localized electron-pair bonding units by using the NBO program[22]. Through this method, the input atomic orbital basis set is transformed via natural atomic orbitals (NAOs) and natural hybrid orbitals (NHOs) into natural bond orbitals (NBOs), which correspond to the localized one centre (“lone pair”) and two-centre (“bond”) elements of the Lewis structure. All possible interactions between “filled” (donor) Lewis-type NBOs and “empty” (acceptor) non-Lewis NBOs orbitals, together with their energetic quantification (stabilization energy), have been obtained by a second-order perturbation theory analysis of the Fock matrix. Only stabilization energy higher than 10 $kcal.mol^{-1}$ has been considered.

3 Results and Discussion

Considered cage-like surface models

Silica surfaces can be natural or synthetic but also crystalline (quartz, cristobalite, edingtonite, ...) or amorphous. In general, except for stishovite who crystallizes in the rutile structure type with silicon in six-fold coordination[23] and pyrogenic silica[24] for which the coordination numbers of silicon can vary from 2 to 6, crystalline and amorphous surfaces consist of inter-linked SiO_4 moiety in a tetrahedral arrangement, with the different silicon atoms interconnected by oxygen bridges, named siloxane bridges. The chemical properties of these silica surfaces are mostly governed by the chemistry of its surface, and most precisely, by the presence of silanol groups. In this way, as aforementioned, the thermal treatment of the surface can strongly modify these properties. One of the most versatile routes for the silica synthesis is the sol-gel one. In a sol-gel process[25], the silica surface is formed by condensation of $Si(OH)_4$ entities obtained by the hydrolysis of sodium silicate or alkoxysilane. The preparation of silica can also take place in anhydrous vapor phase at high temperature, for example, vaporizing SiO_2 in an arc of plasma jet and condensing it in stream of dry inert gas[26]. The silanol groups are very reactive and will be involved in interactions and chemical reactions at the silica surface. For this reason, it is necessary to determine the number of silanol groups on the silicate surface. Despite the complexity of the silica surface, several experimental studies have been carried out for that purpose: Raman spectroscopy[27], thermogravimetric analysis[28], Karl Fischer titration[29] or other chemical methods[30]. Zhuravlev[9a] has shown that in average the OH coverage, for a thermal treatment at temperature less than 200°C is a constant equal to 4.6 ± 0.5 $OH.nm^{-2}$, regardless of the origin and structural characteristics for a set of about 100 different silica samples.

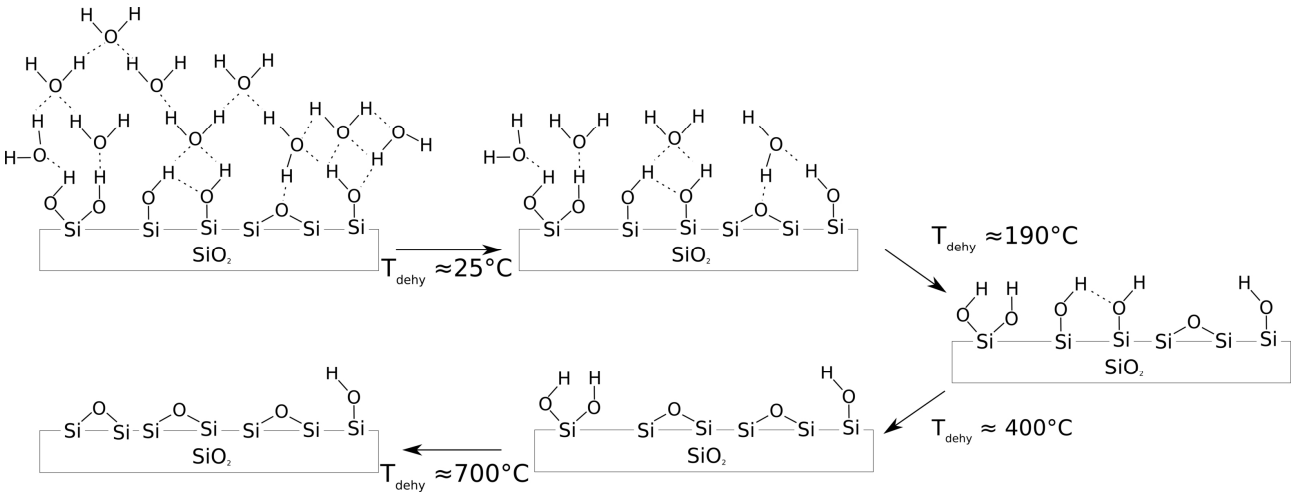

Figure 3. Schematic representation of the conclusions of the Zhuravlev model[31].

This study is based on an exchange reaction between hydrogen and deuterium atoms monitored by mass spectroscopy. This method has the advantage that only the surface silanols are taken into account, and not the subsurfacic silanols or adsorbed water. Moreover, combining the Zhuravlev

model with IRTF integration (integration of the surface of each vibration band corresponding to the silanol groups) and MAS ^{29}Si NMR data, it is possible to obtain the proportion of each type of silanol group as a function of the temperature. As nicely shown by Zhuravlev[31], at room temperature (T_{dehy} < 25°C), all the different types of silanol groups coexist, at a maximum concentration of 4.6 ± 0.5 OH.nm^{-2}. At this temperature the silica surface is also covered by different layers of physically adsorbed water (see figure 3). The reversible dehydration reaction (removal of physically adsorbed water) takes place by raising the temperature to 25 – 190°C. From 190°C, the dehydration reaction is complete and any physically adsorbed water is desorbed while the silanol surface coverage remains constant and equal to 4.6 ± 0.5 OH.nm^{-2}, with a 1.15/2.85/0.60 isolated/vicinal/geminal ratio. The thermal treatment of the surface above 190°C leads to the dehydroxylation of the silica surface or the condensation of neighboring silanol groups to form water and siloxane bridges. This process leads to a decrease of the silanol density as a function of the temperature. In order to describe the presence of different silanol groups onto a $SiO_{2\text{-}200}$ surface (isolated, vicinal, germinal or a mixture of vicinal and germinal silanol groups), and in continuation of previous theoretical studies, five cage-like molecular models (Figure 4) were defined. In all cases, two silicon atoms represent the emerged part of the silica surface and thus of the different silanol groups. The emerged part is surrounded by a layer built around four silicon atoms, themselves connected to O–SiH_3 groups which are chosen as model to mimic the continuity of the surface. Finally, a second layer formed by two silicon atoms, connected by a siloxane bridge, is added to increase the rigidity of the model. Both silicon atoms are connected to hydroxyl groups in order to saturate the model. In a same way, SiH_3 groups are added, on the emerged part of the silica, to saturate the lateral siloxane bridges formed during the dehydroxylation reaction of the silica surface.

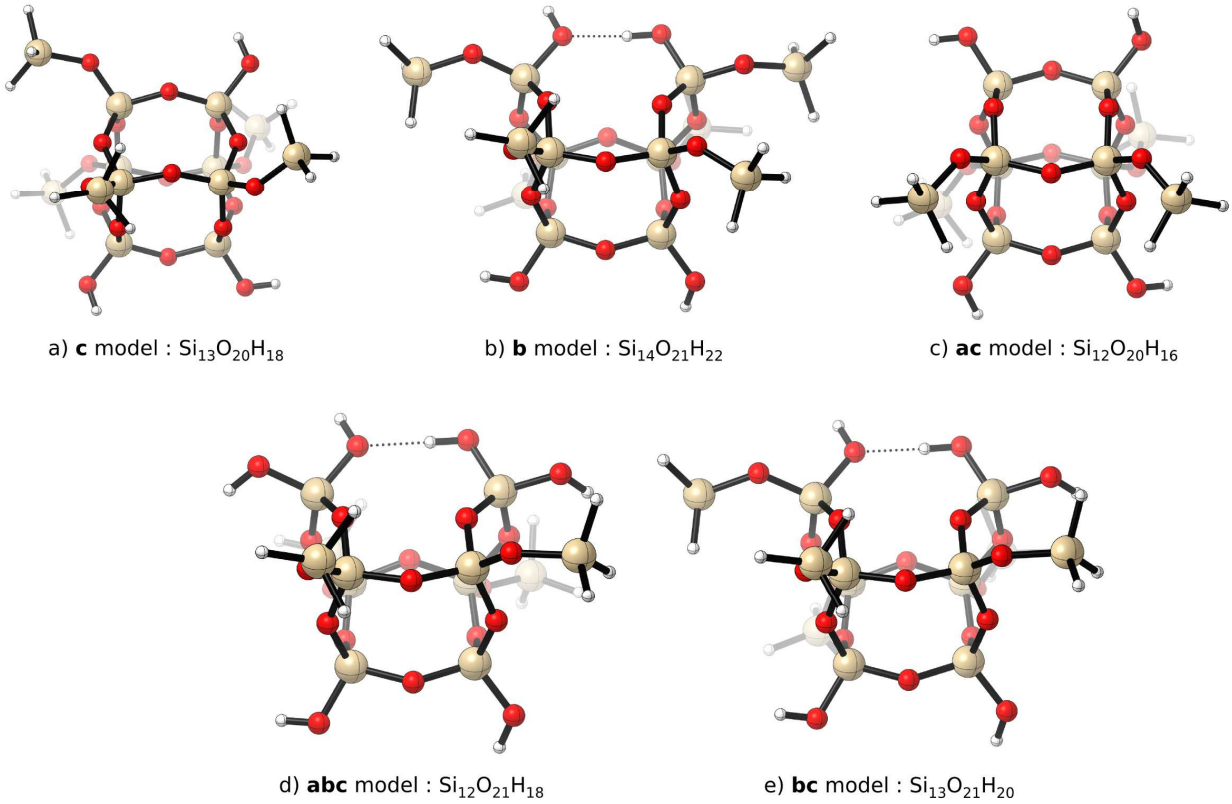

Figure 4. Representation of the five systems, with different silanol groups, used as model of a silica surface dehydroxylated at 200°C

Could these five models be considered relevant models of a $SiO_{2\text{-}200}$ surface? A partial answer should be given by comparing experimental[32,9d] and calculated vibrational frequencies of the hydroxyl groups. IR spectroscopy studies show that under air before the dehydroxylation treatment, the OH stretching frequency of adsorbed water molecules is dominant between 3000 and 3750 cm^{-1}. At 190°C, the dehydration reaction is complete and any physically adsorbed water is desorbed. In this case, the sharp band at 3747 cm^{-1}, assigned to isolated silanols, becomes stronger and more distinct. The vibrational frequencies associated with the geminal and vicinal hydroxyl groups lie between 3500 and 3747 cm^{-1}, the lowest values corresponding to silanols involved in hydrogen bonds.

Table 1. Calculated values for the vibrational frequencies (in cm^{-1}) of the OH groups for the different surface models

Model	$\nu_{O\text{-}H}$	type of silanol
ac	3771 / 3769	vicinal

c	3770	isolated
b	3763	vicinal
	3516	vicinal H-bonded
abc	3757/ 3767 / 3772	geminal
	3518	geminal H-bonded
bc	3771	geminal
	3516	geminal H-bonded
	3760	vicinal

As can be seen in table 1, the calculated ν_{OH} of an isolated silanol, 3770 cm^{-1} in **c** model, is in good agreement with the experimental value of 3747 cm^{-1}. It is noteworthy that the calculated ν_{OH} for two silanol groups in vicinal position linked by a siloxane bridge (**ac** model), are almost identical to those calculated for an isolated silanol group (**c** model), 3771 cm^{-1} and 3769 cm^{-1} *vs.* 3770 cm^{-1}. Models **b**, **abc** and **bc** presents one OH stretching frequency around 3518 cm^{-1} corresponding to a hydroxyl group involved in a hydrogen bond. Likewise, in agreement with experimental observation the OH stretching frequencies of geminal and vicinal silanols, *i.e.*, **abc**, **bc** and **b** models, are calculated to be close to the ν_{OH} of an isolated silanols, between 3772 and 3757 cm^{-1}. Thus, these three types of silanols are indistinguishable on a $SiO_{2\text{-}200}$ IR spectrum. As a consequence, the five cage-like molecular clusters are in agreement with experimental IR data.

Table 2. Comparison between the Theoretical and the Experimental ^{29}Si NMR Chemical Shifts for the different silanol groups. Chemical shifts are given with respect to TMS (theoretical chemical shielding: 352.9 ppm)

Silicon atoms	isolated	vicinal	geminal	Siloxane
Exp. ^{29}SI NMR	-99	-99	-90	-109
ac	-91.0 / -90.9	-	-	-98.7
c	-90.8	-	-	-98.4

b	-	-86.0	-	-96.7
abc	-	-	-77,3	-96.4
bc	-	-87.8	-74.3	-96.4

Another powerful source of information is NMR spectroscopy, as it concerns both ^{1}H and ^{29}Si nuclei[33,9e]. ^{1}H and ^{29}Si NMR has become a standard method to structurally characterize the silicates and silica polymorphs. With respect to tetramethylsilane in ^{1}H NMR, both isolated and geminal silanols have a chemical shift ($\delta(^{1}H)$) of 2.0 ppm whereas those interacting via H-bonds on hydrated samples show a $\delta(^{1}H)$ in the range 3 – 5 ppm. Concerning the ^{29}Si MAS-NMR, the observed signal around -109 ppm is assigned to the Q^4 atoms whereas the silicon atoms with a chemical shift around -99 ppm are attributed to the Q^3 silanols, *i.e.*, vicinal or isolated silanols. Finally, the signal at -90 ppm arise from geminal silanols corresponding to a Q^2 environment for the silicon atom. Thus, ^{29}Si MAS-NMR spectroscopy does not allow to discriminate between isolated and vicinal silanols, since their resonances are similar around $\delta(^{29}Si)$ = -99 ppm. Nevertheless, they can be distinguished from silicon atoms involved in siloxane bonds or geminal silanols, which are respectively more shielded by 10 ppm ($\delta(^{29}Si)$ = -109 ppm) and less shielded by 9 ppm ($\delta(^{29}Si)$ = -90 ppm). The relevance of our five cage-like $SiO_{2\text{-}200}$ surface models was checked by comparing the experimental ^{1}H and ^{29}Si NMR isotropic chemical shift with the calculated values (Table 2). The ^{29}Si NMR chemical shifts calculated for our models are in the -74.3 to -77.3 ppm range for geminal silanols, -86.0 to -87.8 ppm for vicinal silanols, -90.8 to -91.0 ppm for isolated silanols and -96.4 to -98.7 for siloxane silicon atoms. Theoretical results are fairly accurate with respect to experimental values with an error lower than 15%. The assignation of the chemical shifts to the different bonding situations is also in good agreement with the reported experimental values, with $\Delta\delta$ around 3 ppm between Q^3 isolated and vicinal silanols, $\Delta\delta$ around 14 ppm between Q^3 and Q^2 silanols and $\Delta\delta$ around -8 ppm between Q^3 silanols and siloxane silicon atoms. The calculated ^{1}H NMR isotropic chemical shifts for hydrogen atoms involved in a hydrogen bond are in the 5.4 to 5.7 ppm range, 2.0 to 2.3 ppm otherwise, which is in good agreement with the aforementioned experimental values. In summary, we obtain the same chemical shielding for isolated and vicinal silanols, whereas silanol groups and siloxane bridges can be differentiated. The five considered models well reproduce the vibrational features of the silanol groups and the $\delta(^{29}Si)$ and $\delta(^{1}H)$ NMR chemical shifts of a $SiO_{2\text{-}200}$ surface. Thus, it is necessary to take all the models into account to study the grafting mode of

$Ln(N(SiMe_3)_2)_3@SiO_{2-200}$.

Grafted lanthanide complexes

Grafting reaction of a Lanthanide complexes on cluster models

To understand the surface chemistry of silica, we will first study the grafting of lanthanide amides $Ln(N(SiMe_3)_2)_3$ Ln=Y, La, Nd, Yb onto silica. As aforementioned (see Figure 1), the grafting reaction occurs through a protonolysis of the Ln-N bond by surface silanols, which generates a covalent ≡Si-O-Ln bond with the concomitant formation of a free hexamethyldisilazane molecule. In a previous work on SiO_{2-700}[11], we have demonstrated that the grafting reaction of $La(N(SiMe_3)_2)_3$ on the **ac** model leading to the formation of a mono-grafted complex, $La(N(SiMe_3)_2)_3$@**ac-1** (figure 5a), is an exergonic process (-32.4 kcal.mol^{-1} with respect to the separated reactants). Subsequently from $La(N(SiMe_3)_2)_3$@**ac-1**, the formation of a bi-grafted specie, $La(N(SiMe_3)_2)_3$@**ac-2** (figure 5c), is predicted to be exergonic with respect to $La(N(SiMe_3)_2)_3$@**ac-1** by -23.8 kcal.mol^{-1}, -56.2 kcal.mol^{-1} with respect to the separated reactants. The formation of $La(N(SiMe_3)_2)_3$@**ac-2** is accompanied by the uptake of the hydrogen atom of the second silanol group by one bis(trimethylsilyl)amido group. The resulting lanthanum complex is bi-coordinated to the surface, with the lanthanum atom in bridging position between two oxygen atoms, and it exhibits a hexamethyldisilazane molecule which makes a hydrogen bond with a siloxane oxygen. This reaction requires a low activation barrier of + 0.6 kcal.mol^{-1} with respect to $La(N(SiMe_3)_2)_3$@**ac-1**. In the present work, in order to evaluate the effect of the metal centre we have considered the grafting reaction of three additional rare-earth silylamides, $Y(N(SiMe_3)_2)_3$, $Yb(N(SiMe_3)_2)_3$ and $Nd(N(SiMe_3)_2)_3$ onto the different silica surface models. As expected[34] and summarized in Table 3, the grafting reaction shows similar behaviour in terms of energetics and structural features independently of the considered metal centre. The structures of the monografted, the bigrafted and the transition states are similar for all the considered metal centres with an average deviation of the Ln – N and Ln – O bond lengths of less than 0.15 Å. In the same way, from an energetic point of view, a distinct metal effect was not observed. For the four different complexes considered in our calculations only a marginal influence of the lanthanide on the activation energy of the bi-grafting process (averaging 3 kcal.mol^{-1}) is found indicating that the reaction is easy and feasible for all the lanthanide centres. The monografted:bigrafted relative Gibbs-free energy difference is also identical, around 28 kcal.mol^{-1}, for the four systems. Therefore, for the sake of clarity, the following discussion is limited to the study of the grafting reaction of the lanthanum complex onto silica.

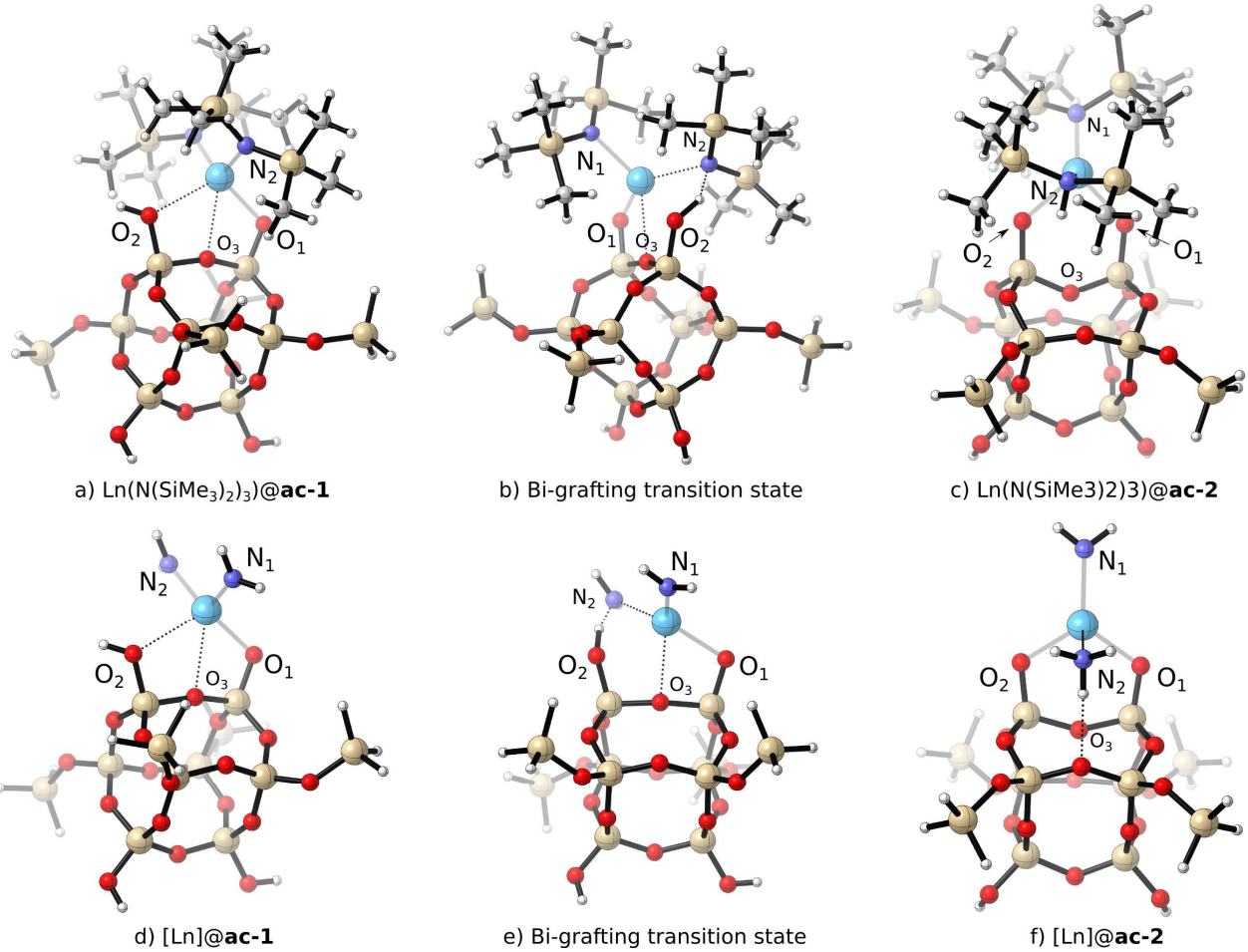

Figure 5. Structures obtained by grafting $Ln(NR_2)_3$ (R = $SiMe_3$ or H) (Ln = La, Y, Yb, Nd) onto the **ac** model.

As we can see on Table 3, the Gibbs-free energy difference between both grafting modes is also very close to that obtained considering a simplified ligand, *i.e.*, by replacing the trimethylsilyl groups by a hydrogen atom, 24.4 *vs.* 28.0 kcal.mol^{-1} for lanthanum and 23.7 *vs.* 28.4 kcal.mol^{-1} for neodymium complexes. Despite our efforts, it has not been possible to locate any minimum energy points corresponding to monografted ytterbium and yttrium species. Geometrically speaking, replacing $SiMe_3$ by H does not significantly influence the structural features of the complex. As expected[35], with the simplest $Ln(NH_2)_3$ complex, the Ln – O bond lengths are found to be systematically longer (average 0.05 Å) whereas the Ln – N bond lengths are shorter (average 0.07 Å). Therefore, in order to save some computational time, the following discussion is limited to the use hydrogen atoms instead of trimethylsilyl groups.

Table 3. Selected structural parameters (distances in Å) and comparison of the Gibbs-free energies (kcal.mol^{-1}) of the grafting reaction of $Ln(NR_2)_3$ (R = $SiMe_3$ or H) (Ln = La, Y, Yb, Nd) on **ac**

model. The labels O_1, O_2, O_3, N_1 and N_2 refer to the intermediates and transition states shown in Figure 5.

	$\Delta_rG°$	Ln – O_1	Ln – O_2	Ln – O_3	Ln – N_1	Ln – N_2	$\Delta_rG°$	Ln – O_1	Ln – O_2	Ln – O_3	Ln – N_1	Ln – N_2
		R= $SiMe_3$						R= H				
La$(NR_2)_3$@**ac-1**	-34.0	2.367	2.886	2.810	2.369	2.370	-34.4	2.392	2.805	2.767	2.300	2.305
Y$(NR_2)_3$@**ac-1**	-33.1	2.189	3.578	2.460	2.181	2.277	-	-	-	-	-	-
Yb$(NR_2)_3$@**ac-1**	-35.0	2.174	3.629	2.397	2.168	2.263	-	-	-	-	-	-
Nd$(NR_2)_3$@**ac-1**	-33.9	2.334	2.752	2.670	2.320	2.338	-34.8	2.336	2.731	2.720	2.250	2.255
TS_{La}	-33.4	2.350	2.770	2.759	2.346	2.494	-40.5	2.336	2.552	2.637	2.282	2.540
TS_Y	-31.0	2.210	2.652	2.502	2.178	2.313	-	-	-	-	-	-
TS_{Yb}	-31.7	2.179	2.961	2.450	2.166	2.279	-	-	-	-	-	-
TS_{Nd}	-30.7	2.294	2.647	2.712	2.288	2.471	-	-	-	-	-	-
La$(NR_2)_3$@**ac-2**	-58.4	2.273	2.278	3.803	2.368	2.776	-62.4	2.295	2.293	3.266	2.306	2.707
Y$(NR_2)_3$@**ac-2**	-60.7	2.120	2.110	3.698	2.201	2.565	-64.8	2.120	2.119	3.373	2.155	2.490
Yb$(NR_2)_3$@**ac-2**	-62.7	2.096	2.094	3.677	2.179	2.522	-65.7	2.100	2.100	3.365	2.136	2.458
Nd$(NR_2)_3$@**ac-2**	-57.6	2.221	2.225	3.775	2.317	2.709	-63.2	2.240	2.240	3.273	2.256	2.640

Before looking at the reaction products between the lanthanum catalyst and the **c** model, we shall underline that it is not possible to obtain hydrogenated ammonia ligands since no vicinal silanol group is present. The grafting reaction similar to [La]@**ac-1** on the **c** model leads to a bridging mono-grafted lanthanum, namely [La]@**c-1** (figure 6), whose formation is exergonic by -32.1 kcal.mol^{-1} with respect to the separated reactants. This mono-grafting is confirmed by a geometrical analysis for instance the La-O distance of 2.393 Å for [La]@**c-1** (2.392 Å for [La]@**ac-1**). The second-order perturbation NBO analysis also reveals the presence of two stabilizing interactions (donation from a lone pair of oxygen atoms towards an empty *d* orbital of the metal centre) between two oxygen atoms of siloxane bridges and the metal centre (for [La]@**c-1**, La-O distance of 2.736 and 2.824 Å) or one oxygen atom of a siloxane bridge and the oxygen atom on the vicinal silanol group and the metal centre ([La]@**ac-1**, La-O distance of 2.767 and 2.805 Å).

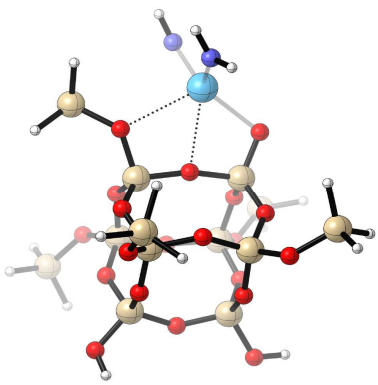

Figure 6. [La]@**c-1** structure obtained by grafting the lanthanum complex onto the **c** model.

In the present work, we have also considered the grafting reaction of $La(NH_2)_3$ on the **b**, **abc** and **bc** models. As aforementioned, these three models allow us to simulate other kinds of silanols (geminal and vicinal silanols) that can be present at the surface of SiO_{2-200} silica. However, even if several attempts to coordinate $La(NH_2)_3$ on these three cage-like models have been considered, the most stable structure is similar in the three cases (see Figure 7). These structures share common features with [La]@**ac-2**. Indeed, in the [La]@**abc-1**, [La]@**bc-1** and [La]@**b-1** structures, the grafting reaction also involves the uptake of the hydrogen atom of a second silanol group by another amino group. The resulting lanthanum complexes are therefore bi-grafted on the surface, with the lanthanum atom in a bridging position between two oxygen atoms ($La\text{-}O_1$ and $La\text{-}O_2$ distances around 2.36 Å), and exhibit an ammonia molecule which remains coordinated to the metal centre. However, contrarily to [La]@**ac-2**, the second-order perturbation NBO analysis reveals that these bi-grafted species are also highly stabilized by the interaction of the metal centre with two additional oxygen atoms ($La\text{-}O_3$ and $La\text{-}O_4$ distances around 2.73 Å) of the silica surface by donation from an oxygen lone pair towards an empty *d* orbital of the metal centre. Thus, this grafting mode induces a partial insertion of the lanthanide atoms onto the SiO_{2-200} silica surface. The formation of [La]@**abc-1**, [La]@**bc-1** and [La]@**b-1** is predicted to be exergonic by -76.4, -77.1 and -75.8 $kcal.mol^{-1}$ with respect to the separated reactants.

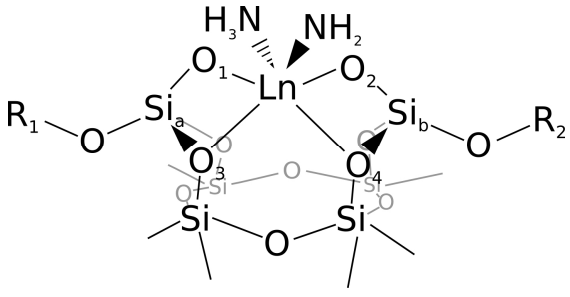

Figure 7. Schematic representation of the most stable structure obtained by the grafting of $La(NH_2)_3$@**b-1** (R_1=R_2=SiH_3), **abc-1** (R_1=R_2=H) and **bc-1** (R_1=SiH_3 and R_2=H) models.

As we can see on Figure 8, the formation of either [La]@**abc-1** or [La]@**bc-1** or [La]@**b-1** takes place through a kinetically accessible and exergonic process. The reaction sequence starts by the protonolysis of the La-N bond by surface silanols, which generates a covalent ≡Si-O-La bond with the concomitant formation of a free ammonia molecule. The lanthanum complex is mono-grafted on

a geminal site (La-O distance of 2.398 Å). As observed on isolated silanol groups, the mono-grafting coordination mode is stabilized by the donation from a lone pair of the second hydroxyl group towards an empty *d* orbital of the metal centre (La-O distance of 2.629 Å). From an energy point of view, the formation of this monografted species is exergonic (-36.2 kcal.mol^{-1} with respect to the separated reactants). This monografted intermediate will thus likely tip over in order to establish a stabilizing interaction with the vicinal silanol and an oxygen atom of a siloxane bridge yielding a more energetically stable intermediate (-46.4 kcal.mol^{-1} with respect to the separated reactants). The bi-grafting reaction which involves the uptake of the hydrogen atom of the silanol group by one of the amine groups can thus proceed with an energy barrier of 8.5 kcal.mol^{-1} with respect to the previous intermediate (-37.9 kcal.mol^{-1} with respect to the separated reactants).

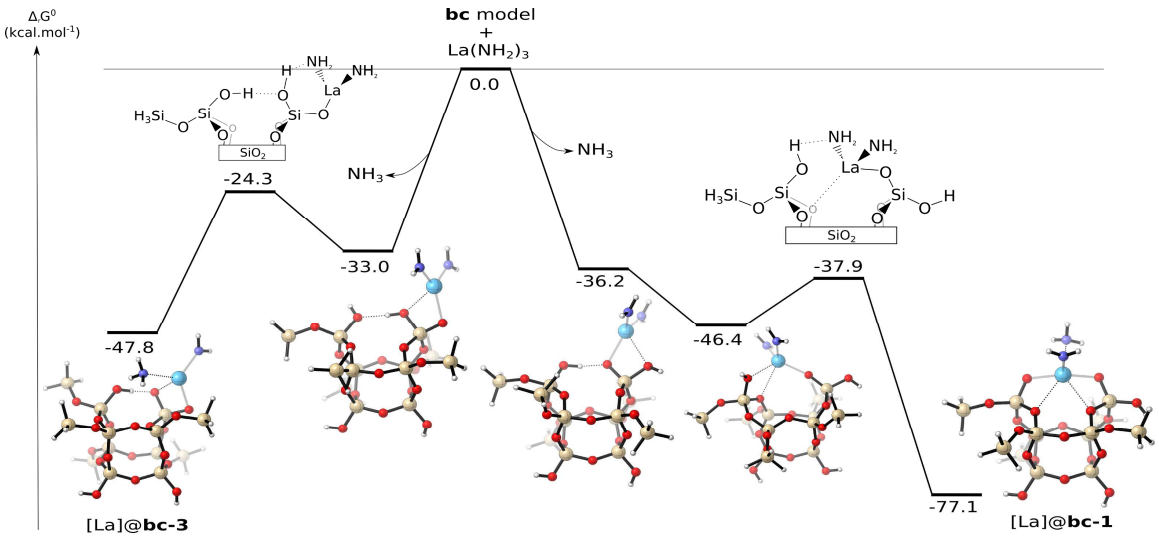

Figure 8. Calculated free-energy profile (in kcal.mol^{-1}) for the grafting reaction of $La(NH_2)_3$ onto the **bc** model.

In the same way, a bigrafted compound on a geminal site, such as [La]@**bc-3** (Figure 8), can also be obtained by grafting $La(NH_2)_3$ on **abc** and **bc** models. As for the bi-grafting reaction on vicinal silanols, this reaction begins by the exergonic (-33.0 kcal.mol^{-1} with respect to the separated reactants) protonolysis of a La-N bond by surface silanols leading to a lanthanum complex mono-grafted on a geminal site (La-O distance of 2.367 Å). The mono-grafting coordination is also stabilized by the donation from a lone pair of the second hydroxyl group of the geminal site towards an empty *d* orbital of the metal centre (La-O distance of 2.617 Å). From this intermediate, the uptake of the hydrogen atom by the amine group takes place through an accessible transition state

(8.7 kcal.mol^{-1} from monografted intermediate, -24.3 kcal.mol^{-1} with respect to the separated reactants), yielding the stable bi-grafted [La]@**bc-3** compound (-47.8 kcal.mol^{-1} with respect to the separated reactants). The resulting lanthanum complexes are therefore bi-grafted on the surface, with the lanthanum atom in a bridging position between the two oxygen atoms of the geminal site (La-O distances of 2.307 and 2.398 Å), and exhibit an ammonia molecule which remains coordinated to the metal centre (La-NH_3 distances of 2.704 Å). Thus, the formation of a bi-grafted compound on geminal site is a kinetically accessible and thermodynamically favorable reaction. However, this reaction is not competitive with respect to the bi-grafting reaction on a vicinal site, for which, even if the activation barriers are similar (8.5 vs. 8.7 kcal.mol^{-1}), the resulting bi-grafted specie is more stable (by 29.3 kcal.mol^{-1}).

Experimentally, it is also been observed[36] and characterized by IR, ^{1}H MAS and ^{13}C CPMAS NMR and EXAFS, that the reaction of $La(N(SiMe_3)_2)_3$ on a silica surface, that has been pretreated at 700°C under vacuum conditions (*i.e.* silica surface with low density of surface silanols, like in the **c** model), leads to $[La(N(SiMe_3)_2)_2@SiO_2]$-type complexes. However, after heating the later material to 500°C, some $[La@SiO_2]$-type complex formation is observed, meaning that the grafted lanthanide complexes are able to break siloxane bridges. From [La]@**c-1** breaking one siloxane bridge leads to the structure [La]@**c-2** (Figure 9). The energy profile for the grafting reaction of $La(NH_2)_3$ onto the **c** model is given in Figure 9. Starting from [La]@**c-1**, the formation of [La]@**c-2** takes place through a multistep pathway in which the transfer of the amine group from lanthanide to a neighboring silicon atom is followed by the activation of a Si – O bond and the concomitant formation of a La – O bond. All our attempts to search for alternative concerted mechanisms failed. The amine transfer proceeds with an energy barrier of 21.6 kcal.mol^{-1} with respect to [La]@**c-1**. This corresponds to the rate-limiting step of the bi-grafting reaction. The product of this step is a transient intermediate, located at +6.4 kcal.mol^{-1} with respect to [La]@**c-1**. On this intermediate, as revealed by the second-order perturbation NBO analysis, the monografted metal centre remains in interaction with the transferred amine group (donation from a lone pair of the nitrogen atom towards an empty *d* orbital of lanthanum). This analysis also reveals the formation of a stabilizing interaction between the metal centre and the oxygen atoms of two siloxane bridges, including the oxygen atom which, in the next step, will be involved in the activation of a Si – O bond. The reaction then proceeds through the activation of a Si – O bond and the concomitant formation of a La – O bond. The activation barrier for this step is +2.4 kcal.mol^{-1} relative to transient intermediate and +8.9 kcal.mol^{-1} with respect to [La]@**c-1**. In [La]@**c-2**, one amino group is directly bound to a silicon atom initially involved in the siloxane bridge. The lanthanum complex can thus be considered as bi-grafted, with two short La-O distances (2.312 and 2.388 Å) but also in interaction with two other oxygen atoms, with two long La-O distances (2.930 and 2.973 Å). The formation of

[La]@**c-2** is found to be exergonic by -36.6 kcal.mol^{-1} with respect to the separated reactants, *i.e.*, 4.5 kcal.mol^{-1} more stable than [La]@**c-1** indicating that the Si-O bond breaking is counterbalanced by the formation of a strong La-O bond. In the same way, the opening of a second adjacent siloxane bridge by the transfer of the second amine group to the silica surface, labeled [La]@**c-3**, could also occur as it is an exergonic reaction, -24.7 kcal.mol^{-1} with respect to [La]@**c-2** (-61.3 kcal.mol^{-1} with respect to the separated reactants). As experimentally observed, ligands loss leads to the insertion of the lanthanide atoms on the silica network. The lanthanide atom is now directly bonded to three oxygen atoms (La-O distances between 2.261 and 2.326 Å) and also interacts with three nearby siloxane bridges (La-O distances between 2.708 and 2.847 Å). In this case, as for the bi-grafting step, the highest energy point of the mechanism corresponds to the transfer of the amine group. The formation of the tri-grafted compound takes place *via* the same multistep pathway defined for the bi-grafting process. The amine transfer involves an activation barrier of 21.9 kcal.mol^{-1}, with respect to [La]@**c-2,** to yield a transient intermediate that lies 18.7 kcal.mol^{-1} above [La]@**c-2**. For this intermediate, as for the bi-grafting reaction, the metal centre remains in interactions with the transferred amine group and a stabilizing interaction is formed between the lanthanum and different oxygen atoms of siloxane bridges. This intermediate evolves to the final [La]@**c-3** tri-grafted product *via* a low energy process with an activation barrier calculated to be +1.8 kcal.mol^{-1} with respect to transient intermediate (+20.5 kcal.mol^{-1} with respect to [La]@**c-2**).

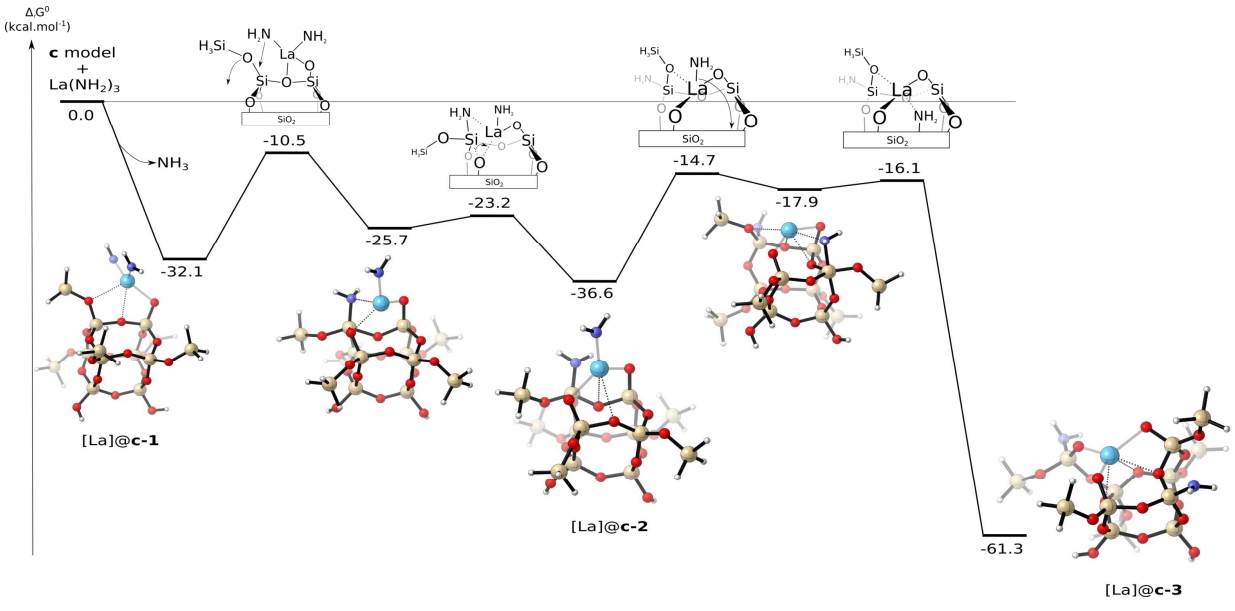

Figure 9. Calculated free-energy profile (in kcal.mol^{-1}) for the grafting reaction of $La(NH_2)_3$ onto the **c** model leading to a trigrafted grafted complex.

From [La]@**abc-1**, [La]@**bc-1** and [La]@**b-1**, the opening of an adjacent siloxane bridge by the transfer of the amino ligands to the silica surface can also take place. The energy profile for the

formation of the tri-grafted [La]@**abc-2**, [La]@**bc-2** and [La]@**b-2** species, taking as example the reaction from [La]@**bc-1**, is given in Figure 10. In this case, the reaction follows the same multistep pathway than for **c** model, i. e., the transfer of the amine group from lanthanide to a neighboring silicon atom is followed by the activation of a Si – O bond and the concomitant formation of a La – O bond. The activation energies for this is reaction are also similar to the one computed for the tri-grafting reaction **c** model. In this case, the activation barrier for the amine transfer lies at +28.8 kcal.mol^{-1} above [La]@**bc-1**. This transition state is 7.2 kcal.mol^{-1} higher than that on **c** model, which is agreement with the greater rigidity of the bi-grafted species on **abc**, **bc** and **b** models due to the partial insertion of the lanthanide atom onto the $SiO_{2\text{-}200}$ silica surface. This transition state yields a transient intermediate, located at +20.7 kcal.mol^{-1} with respect to [La]@**bc-1**, in which, as on **c** model, the metal centre remains in interaction with the transferred amine group. This intermediate evolves *via* an accessible transition state (+21.7 kcal.mol-1 with respect to [La]@**bc-1**) corresponding to the aforementioned activation of a Si – O bond and the formation of a La – O. These exergonic reactions, by roughly -14 kcal.mol^{-1} with respect to [La]@**abc-1**, [La]@**bc-1** and [La]@**b-1**, lead to the formation of respectively [La]@**abc-2**, [La]@**bc-2** and [La]@**b-2** (Figure 10). These complexes, unlike [La]@**c-3**, are tri-grafted and inserted on the silica network, but also exhibit an ammonia molecule which remains coordinated to the metal centre. From a geometrical point of view, the lanthanide atom is directly bonded to three oxygen atoms (La-O distances between 2.337 and 2.361 Å) and also interacts with three nearby siloxane bridges (La-O distances between 2.629 and 2.904 Å). The NBO analysis of [La]@**abc-2**, [La]@**bc-2** and [La]@**b-2** confirms the presence of a stabilizing interaction between three oxygen atoms of different siloxane bridges and the metal centre (donation from a lone pair of these oxygen atoms towards an empty *d* orbital of the metal centre).Thus, independently of the initial grafting mode, the formation of a tri-grafted specie is computed to be a kinetically accessible and thermodynamically favourable process. This is in line with the experimental observation that for silica treated at high temperature, either mono-grafted or tri-grafted compounds could be obtained.

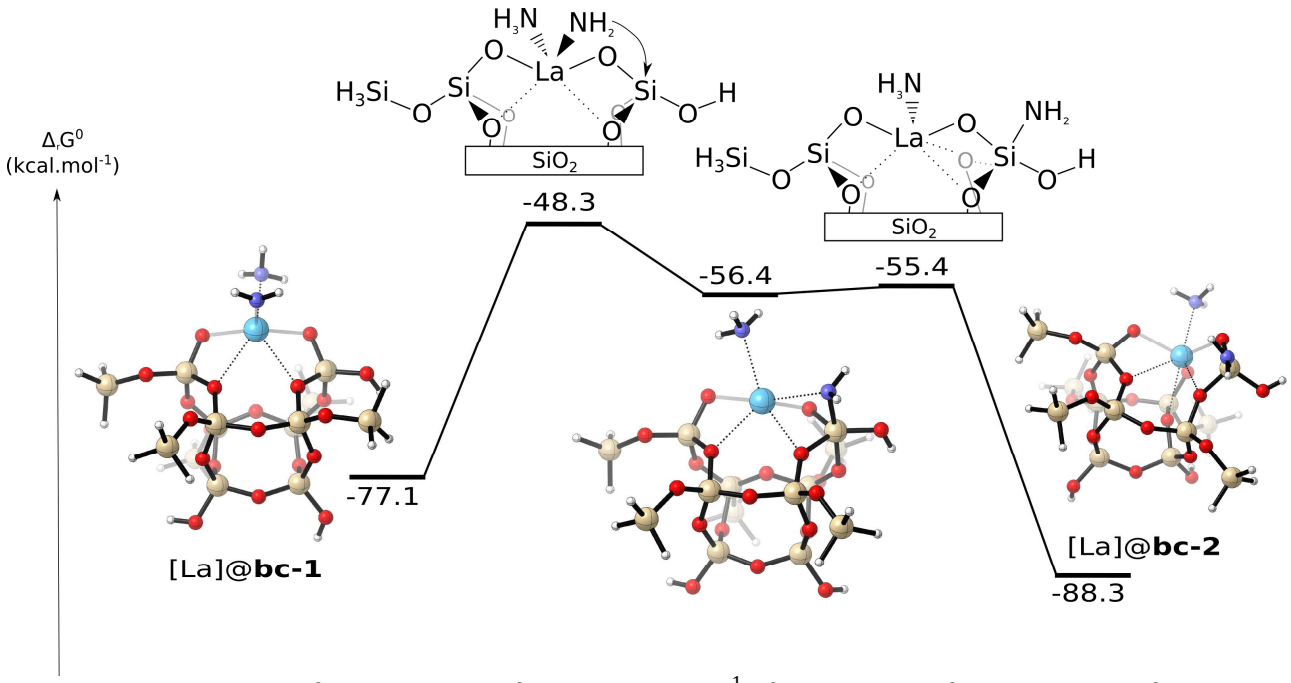

Figure 10. Calculated free-energy profile (in kcal.mol^{-1}) for the tri-grafting reaction of $La(NH_2)_3$ onto the **bc** model from [La]@**bc-1**.

To summarize, the nature of the silanol groups at the silica surface has a great influence on the geometry and stability of the grafted complexes, especially in determining the grafting mode of $La(NH_2)_3$. For instance, the presence of isolated silanol groups leads to the formation of mono-grafted complexes whereas the presence of vicinal silanol groups induces the formation of bi-grafted species (in this case the mono-grafted species evolves into the bi-grafted one by reaction with the neighboring silanol). When the two vicinal silanol are connected by an oxygen atom, the resulting lanthanum complex is bi-grafted to the surface, with lanthanum atom in a bridge position between two oxygen atoms, whereas when the two silanols are H-bonded, the resulting lanthanum complexes are bi-grafted with a lanthanum bonded to two oxygen atoms, but also interacting with two nearby siloxane oxygen atoms. In the same way, a monografted specie can be obtained by the reaction of $La(NH_2)_3$ on a geminal silanols. Finally, from these different structures, tri-grafted species can also be obtained by the opening of one or two adjacent siloxane bridge. In terms of Gibbs Free energy, all reactions are exergonic with respect to the entrance channel, with Δ_rG^0 ranging from -30 to -91 kcal.mol^{-1}. These results qualitatively agree with the experimental data, for the propensity of grafting lanthanide complexes onto SiO_2 surfaces. Thus, it is possible that all the $La(NH_2)_3$ grafting modes coexist so that it could be necessary to consider all the species in future reactivity studies which would involve such complexes.

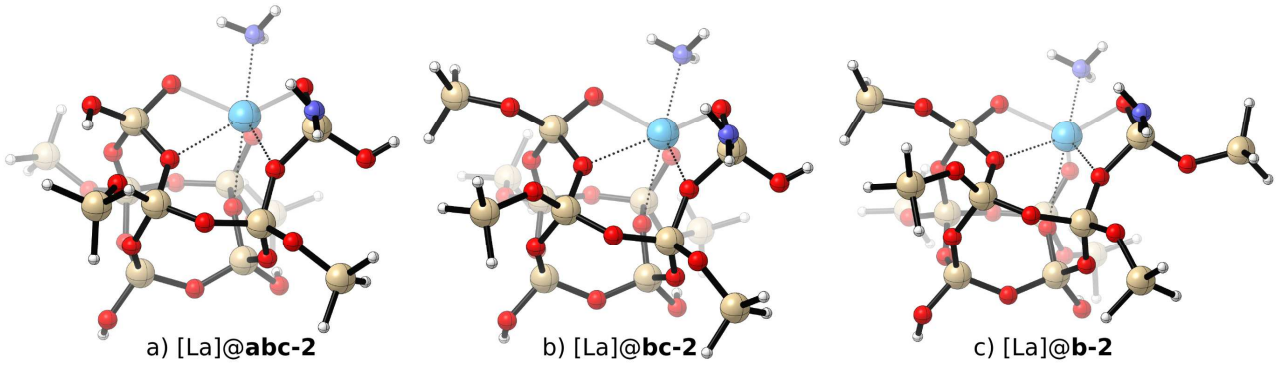

Figure 11. Structures obtained by the opening of one siloxane bridges from bi-grafted [La]@**abc-1**, [La]@**bc-1** and [La]@**b-1** species.

Could the properties of the different grafting modes be distinguished by the coordination of a probe molecule?

In this work, we have considered as probe molecule the triphenylphosphine oxide ($O=PPh_3$) as it is known to react with homogeneous and grafted rare-earth hexamethyldisilylamides, leading to the formation of $[Ln(NR_2)x(O=PPh_3)]$ monoadducts (x = 3 for homogeneous compounds[37] and x = 2 or 1 for grafted systems[5c]). From an experimental point of view, the coordination of the $OPPh_3$ Lewis base has been used to quantify the acidity of multiple sites on a surface. As evidenced by Drago et al.[38], a positive ^{31}P NMR chemical shift difference between free and coordinated $OPPh_3$ is indicative of the coordination to an acidic site and the magnitude of this difference is correlated to the strength of the interaction. Gauvin *et al.*[5c] have shown that reaction of $OPPh_3$ with grafted rare-earth amides onto a SiO_{2-700} surface is reversible as $OPPh_3$ sublimes away upon heating under vacuum. It indicates a certain degree of lability and therefore, to some extent, shows that $OPPh_3$ coordination strength can be affected by the coordination sphere of the grafted complex. It was also shown that this reaction leads to the formation of $[(\equiv Si\text{-}O)\text{-}Ln(NR_2)_2(O=PPh_3)]$, which have been characterized by IR and NMR. $OPPh_3$ has a clear vibrational ($C\text{-}H_{Ph}$, $C\text{-}C_{Ph}$ and O=P) and spectroscopic (^1H, ^{13}C and ^{31}P) signature, which allowed us to carry out the comparison between theoretical and experimental data. Thus, we have considered the coordination of $OPPh_3$ on the different grafted complexes. The NBO analysis reveals that the coordination takes place through the donation from a lone pair of the oxygen atom of $OPPh_3$ towards an empty d orbital of the metal centre. In all cases the coordination of $OPPh_3$ is predicted to be exergonic whatever the considered grafted complex. As mentioned in a previous work, the coordination of $OPPh_3$ on [La]@**ac-1**, [La]@**ac-2**, [La]@**c-1** is a thermodynamically favorable process, with Gibbs-free energies equal to -9.7, -18.0 and -14.6 kcal.mol^{-1} respectively. OPPh3 coordination on the bi-grafted [La]@**abc-1**, [La]@**bc-1** and [La]@**b-1** species is also exergonic by -3.2, -4.5 and -6.9 kcal.mol^{-1} as well as on the mono-grafted compound [La]@**bc-3**, by -12.9 kcal.mol^{-1}. The coordination of OPPh3 on the tri-

grafted species follows the same trend with Gibbs-free energies equal to -18.9, -20.9, -6.6, -8.0 and -8.4 kcal.mol^{-1} respectively for [La]@**c-2**, [La]@**c-3**, [La]@**abc-2**, [La]@**bc-2** and [La]@**b-2**.

Grafted Complex	vibrational frequencies			NMR			
	$\nu(C\text{-}H)_{Ph}$	$\nu(C\text{-}C)_{Ph}$	$\nu(O=P)$	$\delta(H)_{Ph}$	$\delta(C)_{Ph}$		δ P
[La]@**ac-1**	[3025-3098]	[1416-1591]	1126	7.9	124.1	128.3	40.9
[La]@**ac-2**	[3071-3100]	[1417-1592]	1152	7.9	124.9	128.8	47.6
[La]@**c-1**	[3068-3095]	[1417-1592]	1118	8.0	124.9	128.7	46.3
[La]@**b-1**	[2965-3101]	[1462-1591]	1118	8.0	124.2	128.8	43.3
[La]@**abc-1**	[2938-3098]	[1464-1592]	1124	8.0	123.9	129.2	45.7
[La]@**bc-1**	[3037-3101]	[1463-1589]	1127	7.9	123.5	129.0	45.0
[La]@**bc-3**	[3021-3098]	[1416-1592]	1128	7.9	124.5	128.5	40.3
[La]@**c-2**	[3068-3107]	[1416-1591]	1121	8.0	125.0	128.6	41.9
[La]@**c-3**	[3043-3102]	[1464-1592]	1113	6.7	122.0	131.8	51.1
[La]@**b-2**	[3023-3104]	[1462-1591]	1123	7.9	124.8	128.9	42.3
[La]@**abc-2**	[3027-3104]	[1463-1589]	1123	7.9	124.6	129.1	42.0
[La]@**bc-2**	[2935-3100]	[1464-1592]	1118	8.0	125.1	128.9	40.4
Exp. [a]	~ 3066	[1440-1593]	[1120-1180][b]	7.4	128.4	132.5	39.1
$OPPh_3$[c]	[3065-3095]	[1416-1592]	1177	7.7	124.7	129.9	25.7

Table 4. Comparison between the theoretical and the experimental vibrational frequencies (in cm^{-1}), ^{1}H, ^{13}C and ^{31}P NMR chemical shifts (in ppm) of $OPPh_3$ molecule coordinated at different grafted lanthanum complex. ^{1}H and ^{13}C chemical shifts are given with respect to TMS (theoretical chemical shielding: 31.64 ppm / 195.35 ppm respectively to ^{1}H and ^{13}C atoms). ^{31}P chemical shifts are given with respect to phosphoric acid (theoretical chemical shielding: 380.6 ppm). [a] Ref. 5c. [b] expected but not detected band. [c] Free $OPPh_3$ ligand.

The calculated vibrational C-H, aromatic-C, and O=P frequencies of the adsorbed $OPPh_3$ molecule are reported in Table 4. The aromatic C-H and C-C stretching vibrations are found in the same range (between 2935 and 3107 cm^{-1} and between 1417 and 1592 cm^{-1}, respectively) whatever the considered grafted species, close to the experimental values of $OPPh_3$@[La]@$SiO_{2\text{-}700}$, ~ 3066 cm^{-1} and [1440-1593] cm^{-1}, respectively. The vibrational stretching mode of O=P bond, experimentally expected (but not observed) between 1120 and 1180 cm^{-1}, is also obtained in this domain for the different grafting modes. As a consequence, it is not possible to distinguish the different grafting modes by studying only this vibrational property. Another way to discriminate the different grafted species is to compare the theoretical and experimental ^{1}H, ^{13}C and ^{31}P NMR chemical shifts of the coordinated $OPPh_3$ molecule, as reported in Table 4. The ^{1}H isotropic chemical shift calculated for

our different grafted species are in the 6.7 to 8.0 ppm range, in good agreement with reported experimental value of 7.4 ppm for $OPPh_3$@[La]@$SiO_{2\text{-}700}$. The experimental ^{13}C CP-MAS spectrum displays two peaks for the aromatic carbons, δ = 128.4 and 132.5 ppm. Our calculations also yield two ranges of chemical shift between 122.0 and 125.1 ppm and between 128.6 and 131.8 ppm whatever the considered grafted species, also in good agreement with experiments. In this case, it is noteworthy that, not only the theoretical and experimental chemical shifts are close, but the difference between the two experimental peaks and the two theoretical ranges are in good agreement, around 4 ppm. Finally, the $\delta(^{31}P)$ chemical shifts calculated for $OPPh_3$ coordinated on the mono- and bi-grafted compounds are in the 40.3 – 47.6 ppm range, close to the experimental value of δ = 39.1 ppm. This range is slightly enlarged by considering the $OPPh_3$ coordination on the tri-grafted complexes, 40.3 – 51.1 ppm. As a consequence, due to the large number of values in this range, it is not possible to distinguish the different grafting modes by studying the ^{31}P NMR chemical shifts of the coordinated $OPPh_3$ molecule, as for ^{1}H and ^{13}C NMR. However, it is noteworthy that, according to the study Drago *et al.*, the computed ^{31}P NMR chemical shift difference pleads for a dissimilar Lewis acidity of the grafted complexes on a $SiO_{2\text{-}200}$ surface, *i.e.*, a slightly different catalytic activity. Work is in progress in order to assess the influence of this change in Lewis acidity in for instance polymerization reactions.

Conclusion

In conclusion, we have studied the grafting of lanthanide silylamide complexes onto dehydroxylated silica at 200°C. After validation, based on the vibrational features of the silanol groups and the $\delta(^{29}Si)$ and $\delta(^{1}H)$ NMR chemical shifts of a $SiO_{2\text{-}200}$ surface, five cage-like molecular models have been considered in order to study the grafting reaction of $Ln(N(SiMe_3)_2)_3$@$SiO_{2\text{-}200}$. The thermodynamics of this grafting reaction has been investigated showing a marginal influence of the considered lanthanide whereas the nature of the silanol groups at the silica surface has a great influence on the geometry and stability of the grafted complexes. The presence of isolated and geminal silanol groups lead to the formation of mono-grafted complexes. However, the presence of vicinal silanol groups induces the formation of bi-grafted species: (*i*) when the two vicinal silanol are connected by an oxygen atom, the resulting lanthanum complex is bi-grafted to the surface, with lanthanum atom in a bridge position between two oxygen atoms; (*ii*) when the two silanols are H-bonded, the resulting lanthanum complexes are bi-grafted with a lanthanum partially inserted onto the silica surface bonded to two oxygen atoms, but also interacting with two nearby siloxane oxygen atoms. Finally, thermodynamically stable tri-grafted species can also be obtained, from these different structures, by the opening of one or two adjacent siloxane bridge.

The coordination of $OPPh_3$ to the possible grafted complexes does not allow discriminating between the plausible grafting modes since all models could explain the IR and NMR signature of the coordinated molecule. However, the relatively large range of the $\delta(^{31}P)$ chemical shifts (around 10 ppm) indicates some possible important in Lewis acidity of the metal centres, depending on the grafting mode. This might have impact on the reactivity and work is in progress in that direction.

Acknowledgements

CalMip is acknowledged for the generous grant of computing time. LM is member of the "Institut Universitaire de France' and also acknowledge the Humboldt Foundation.

References ans Notes

† Electronic Supplementary Information (ESI) available: Cartesian coordinates and free Gibbs energy for all the intermediates.

[1] (a) J. Fiksel, *Design for Environment: Creating Eco-Efficient Products ans Processes*; McGraw-Hill: New York 1998; (b) *Green Engineering*; Anastas, P. T., Heine, L., Williamson, T. C., Eds.; American Chemical Society: Washington, DC, 2000; (d) P. T. Anastas and J. B. Zimmerrman, *Environ. Sci. Technol.*, 2003, 37(5), 95 – 101.

[2] (a) R. K. Iler, R. K. *The Chemistry of Silica*, 2nd ed.; John Wiley & Sons, Inc.: New York, Chichester, Brisbane, Toronto, 1979; (b) A. P. Legrand, A. P. *The Surface Properties of Silicas*; Wiley, Inc.: New York, 1998; (c) V. Y. Davydov, *In Adsorption on Silica Surfaces*; E. Papirer, Ed.; CRC Press, Taylor & Francis Group: Santa Barbara, CA, 2000; Vol. 90, p 63; (d) A. Rimola, D. Costa, M. Sodupe, J.-F. Lambert and P. Ugliengo, *Chem. Rev.*, 2013, 113, 4216 – 4313.

[3] (a) J.-M. Basset, R. Psaro, D. Roberto, R. Ugo, 2009, Modern Surface Organometallic Chemistry; (b) P. Sautet, F. Delbecq, *Chem. Rev.*, 2010, 110, 1788–1806.

[4] (a) T. J. Woodman, Y. Sarazin, G. Fink, K. Hauschild, M. Bochmann, *Macromolecules*, 2005, 38, 3060. (b) R. M. Gauvin, T. Chenal, R. A. Hassan, A.Addad, A. Mortreux, *J. Mol. Catal. A: Chem.* 2006, 257, 31 ; (b) R. M. Gauvin, A. Mortreux, *Chem. Commun*. 2005, 1146 ; (c) K. Tortosa, T. Hamaide, C. Boisson, R. Spitz, *Macromol. Chem. Phys.* 2001, 202,1156.

[5] (a) G. Gerstberger, R. Anwander, *Microporous Mesoporous Mater.* 2001, 44-45, 303; (b) G. Gerstberger, C. Palm, R. Anwander, *Chem. Eur. J.* 1999, 5, 997 ; (c) R. M. Gauvin, L. Delevoye, R.

A. Hassan, J. Keldenich, A. Mortreux, *Inorg. Chem.* 2007, 46, 1062 ; (d) E. Le Roux, Y. Liang, M. P. Storz, R. Anwander, *J. Am. Chem. Soc.*, 2010, 132, 16368.

[6] R. Anwander, R. Roesky, *J. Chem. Soc., Dalton Trans.* 1997, 137 – 138.

[7] E. Le Roux, R. Anwander, *Surface Organolanthanide and Actinide Chemistry*; Wiley-VCH Verlag GmbH & Co. KGaA, 2009.

[8] R. Anwander, O. Runte, J. Eppinger, G. Gestberger, H. Herdtweck, M. Spiegler, *J. Chem. Soc., Dalton Trans.* 1998, 5, 847–858.

[9] (a) L. T. Zhuravlev, *Colloids Surf.*, A 2000, 173, 1 ; (b) L. T. Zhuravlev, *Langmuir* 1987, 3 ; (c) J. Trebosc, J. W. Wiench, S. Huh, V. S. Lin, M. J. Pruski, *J. Am. Chem. Soc.* 2005, 127, 3057 ; (d) A. Burneau, J. P. Gallas, *In The Surface Properties of Silicas*; A. P. Legrand, Ed.; John Wiley & Sons: Chichester, 1998; pp 145 – 234 ; (e) G. Engelhardt, D. Michel, *High Resolution Solid State NMR of Silicates and Zeolites*; Wiley & Sons: New York, 1987.

[10] (a) R. Anwander, H. W. Görlitzer, G. Gerstberger, C. Palm, O Runte, M. Spiegler, *J. Chem. Soc., Dalton Trans.* 1999, 3611 – 3615 ; (b) K. tortosa, T. Hamaide, C. Boisson, R. Splitz, *Macromol. Chem. Phys.*, 2011,202, 1156 – 1160 ; (c) R. Anwander, *Chem. Mater.*, 2001, 13, 4419 – 4438 ; (d) Y. Chen, Z. Zhy, J. Zhang, J. shen, X. Zhou, *J. Organomet. Chem.*, 2005, 3873 – 3789.

[11] I. Del Rosal, I. C. Gerber, R. Poteau, L. Maron, *J. Phys. Chem. A* 2010, 114, 6322–6330.

[12] X. Rozanska, F. Delbecq, P. Sautet, *Phys ; Chem. Chem. Phys.* 2010, 12, 14930 – 149140.

[13] (a) J. Sauer, P. Ugliengo, E. Garrone, V. R. Saunders, *Chem. Rev.* 1994, 94, 2095 ; (b) M. A. Zwijnenburg, C. van Alsenoy, T. J. Maschmeyer, *Phys. Chem. A* 2002, 106, 12376–12385 ; (c) J.-M Antonietti, M. Michalski, U. Heiz, H. Jones, K. H. Lim, N. Rösch, A. D. Vitto, G. Pacchioni, *Phys. ReV. Lett.* 2005, 94, 213402 ; (d) B. Rhers, A. Salameh, A. Baudoin, E. A. Quadrelli, M. Taoufik, C. Copéret, F. Lefebvre, J.-M. Basset, X. Solans-Monfort, O. Eisenstein, W. W. Lukens, L. P. H. Lopez, A. Sinha, R. R. Schrok, *Organometallics* 2006, 25, 3554–3557 ; (e) F. Blanc, J.-M. Basset, C. Copéret, A. Sinha, Z. J. Tonzetich, R. R. Schrock, X. Solans-Monfort, E. Clot, O. Eisenstein, A. Lesage, L. J. Emsley, *J. Am. Chem. Soc.* 2008, 130, 5886–5900 ; (f) B. Civalleri, E. Garrone, P. Ugliengo, *Chem. Phys. Lett.* 1999, 299, 443–450.

[14] (a) F. VigneMaeder, P. Sautet, *J. Phys. Chem. B* 1997, 101, 8197–8203 ; (b) B. Civalleri, P. Ugliengo, *J. Phys. Chem. B* 2000, 104, 9491 ; (c) R. V. Ginhoven, H. Hjalmarson, A. Edwards, B. Tuttle, *Nucler. Inst. Met. Phys. Res. B* 2006, 250, 274–278; (d) T. P. M. Goumans, A. Wander, C. R. A. Catlow, W. Brown, *A. Mon. Not. R. Astron. Soc.* 2007, 382, 1829 ; (e) T. P. M. Goumans, C. R. A. Catlow, W. A.Brown, *J. Chem. Phys.* 2008, 128, 134709 ; (f) (d) P. Ugliengo, M. Sodupe, F. Musso, I. J. Bush, R. Orlando, R. Dovesi, *Adv. Mater.* 2008, 20, 4579 ; (g) F. Tielens, C. Gervais, J. F. Lambert, F. Mauri, D. Costa, *Chem. Mater.* 2008, 20, 3336.

[15] X. Solans-Monfort, J.-S. Filhol, C. Copéret, O. Eisenstein, *New. J. Chem.* 2006, 30, 842–850.

[16] M. J. Frisch, G. W. Trucks, H. B. Schlegel, G. E. Scuseria, M. A. Robb, J. R. Cheeseman, J. A. Montgomery, Jr., T. Vreven, K. N. Kudin, J. C. Burant, J. M. Millam, S. S. Iyengar, J. Tomasi, V. Barone, B. Mennucci, M. Cossi, G. Scalmani, N. Rega, G. A. Petersson, H. Nakatsuji, M. Hada, M. Ehara, K. Toyota, R. Fukuda, J. Hasegawa, M. Ishida, T. Nakajima, Y. Honda, O. Kitao, H. Nakai, M. Klene, X. Li, J. E. Knox, H. P. Hratchian, J. B. Cross, V. Bakken, C. Adamo, J. Jaramillo, R. Gomperts, R. E. Stratmann, O. Yazyev, A. J. Austin, R. Cammi, C. Pomelli, J. W. Ochterski, P. Y. Ayala, K. Morokuma, G. A. Voth, P. Salvador, J. J. Dannenberg,
V. G. Zakrzewski, S. Dapprich, A. D. Daniels, M. C. Strain, O. Farkas, D. K. Malick, A. D. Rabuck, K. Raghavachari, J. B. Foresman, J. V. Ortiz, Q. Cui, A. G. Baboul, S. Clifford, J. Cioslowski, B. B. Stefanov, G. Liu, A. Liashenko, P. Piskorz, I. Komaromi, R. L. Martin, D. J. Fox, T. Keith, M. A. Al-Laham, C. Y. Peng, A. Nanayakkara, M. Challacombe, P. M. W. Gill, B. Johnson, W. Chen, M. W. Wong, C. Gonzalez, and J. A. Pople, *Gaussian 03*, *revision E.01* ; Gaussian, Inc : Wallingford, CT, 2003.

[17] (a) J. P. Perdew, *Unified Theory of Exchange and Correlation Beyond the Local Density Approximation. In Electronic Structure of Solids*; J. P. Ziesche, H. Eschrig, Eds.; Akademie: Berlin, 1991 ; (b) J. P. Perdew, K. Burke, Y. Wang, *Phys. Rev. B* 1996, 54, 16533− 16539 ; (c) C. Burke, J. P. Perdew, Y. Wang, *Derivation of a Generalized Gradient Approximation: The PW91 Density Functional. In Electronic Density Functional Theory: Recent Progress and New Directions*; J. F. Dobson, G. Vignale, M. P. Mas, Eds.; Plenum: New York, 1998 ; (d) J. P. Perdew, J. A. Chevary, S. H. Vosko, K. A. Jackson, M. R. Pederson, D. J. Singh, C. Fiolhais, *Phys. Rev. B* 1992, 46, 6671−6687 ; (e) J. P. Perdew, K. Burke, Y. Wang, *Phys. Rev. B* 1998, 57, 14999−15033 ; (f) J. P. Perdew, J. A. Chevary, S. H. Vosko, K. A. Jackson, M. R. Pederson, D. J. Singh, C. Fiolhais, *Phys. Rev. B* 1993, 48, 4978−4978.

[18] (a) M. Dolg, H. Stoll, H. J. Preuss, *Chem. Phys.* 1989, 90,1730−1734 ; (b) X. Cao, M. Dolg, *J. Mol. Struct.:THEOCHEM* 2002, 581, 139−147.

[19] (a) P. C. Hariharan, J. A. Pople, *Theor. Chim. Acta* 1973, 28, 213−222 ; (b) W. J. Hehre, R. Ditchfield, J. A. Pople, *J. Chem. Phys.* 1972, 56, 2257−2261.

[20] (a) F. J. London, *J. Phys. Radium* 1937, 8, 397–409 ; (b) R. McWeeny, *Phys. Rev.* 1962, 126, 1028–1034 ; (c) R. Ditchfield, *Mol. Phys.* 1974, 27, 789–807 ; (d) J. L. Dodds, R. McWeeny, A. Sadlej, *J. Mol. Phys.* 1977, 34, 1779–1791;

[21] (a) H. Staub, I. Del Rosal, L. Maron, F. Kleitz, F.-G. Fontaine, *J. Phys. Chem. C*, 2012, 116, 25919−25927 ; (b) N. Merle, J. Trébosc, A. Baudouin, I. Del Rosal, L. Maron, K. Szeto, M. Genelot, A. Mortreux, M. Taoufik, L. Delevoye, R. M. Gauvin, *J. Am. Chem. Soc.*, 2012, *134*, 9263–9275 ; (c) N. Merle, G. Girard, N. Popoff, A. De Mallmann, Y. Bouhoute, J. Trébosc, E. Berrier, J.-F. Paul, C. P. Nicholas, I. Del Rosal, L. Maron, R. M. Gauvin, L. Delevoye, M. Taoufik, *Inorg. Chem.* 2013, 52, 10119−10130 ; (c) Y. Bouhoute, A. Garron, D. Grekov, N. Merle, K. C. Szeto, A. De Mallmann, I. Del Rosal, L. Maron, G. Girard, R. M. Gauvin, L. Delevoye, M. Taoufik, *ACS Catal.* 2014, 4, 4232−4241 ; (e) N. Popoff, J. Espinas, J. Pelletier, B. Macqueron, K. C. Szeto, O. Boyron, C. Boisson, I. Del Rosal, L. Maron, A. De Mallmann, R. M. Gauvin, M. Taoufik, *Chem. Eur. J.*, 2013, 19, 964–973 ;

[22] (a) A. E. Reed, F. J. Weinhold, *Chem. Phys.* 1983, 78, 4066 – 4074 ; (b) A. E. Reed, L. A. Curtiss, F. Weinhold, *Chem. Rev.* 1988, 88, 899−926.

[23] O. W. Flörke, H. A. Graetsch, F. Brunk, L. Benda, S. Paschen, H. E. Bergna, W. O. Roberts, W. A. Welsh, C. Libanati, M. Ettlinger, D. Kerner, M. Maier, W. Meon, R. Schmoll, H. Gies, D. Schiffmann, 2008. Silica. Ullmann's Encyclopedia of Industrial Chemistry.

[24] V. D. Khavryuchenko, O. V. Khavryuchenko, V. V. Lisnyak, Critical Reviews in Solid State and Materials Sciences, 2011, 36, 47-65.

[25] a) D. Barby, Silicas, in « Characterization of Powder Surfaces », G. D. Parfitt and G. S. W. Sings eds., Academic Press, London , UK, 1976 , 353 ; (b) R. K. Iler, The Chemistry of Silica, John Wiley

& Sons, New York, 1979 ; (c) K. K. Unger, « Porous Silica, its properties and use as a support in column liquid chromatography », Elsevier, Amsterdam, The Netherlands, 1979 ; (d) W. Stöber, A. Fink, E. Bohm, *J. Coll. Interface Sci.*, 1968, 26, 62 – 69 ; (e) A. M. Buckley, M. Greenblatt, *J. Chem. Educ.*, 1994, 71, 599 – 602.

[26] *Adsorption on Silica Surfaces*; E. Papirer, Ed.; Marcel Dekker Inc.: New York, 2000; Vol. 90.

[27] (a) B. J. Humbert, *Non-Cryst. Solids* 1995, 191, 29–37 ; (b) J. Gnado, P. Dhamelincourt, C. Pélégris, M. Traisnel, A. L. M. Mayot, *Non-Cryst.Solids* 1996, 208, 247–258 ; (c) T. Czuryszkiekiewicz, J. Ahvenlammi, P. Kortesuo, M. Ahola, F. Kleitz, M. Jokinen, M. Linden, J. B. Rosenholm, *J. Non-Cryst. Solids* 2002, 306, 1–10.

[28] (a) A. P. Legrand, H. Hommel, A. Tuel, A. Vidal, H. Balard, E. Papirer, P. Levitz, M. Czernichowski, R. Erre, H. V. Damme, *AdV. Colloid Interface Sci*. 1990, 33, 91–330 ; (b) R. Mueller, H. K. Kammler, K. Wegner, S. E. Pratsinis, *Langmuir* 2003, 19, 160–165.

[29] (a) K. Fischer, *Angew. Chem., Int. Ed. Eng.* 1935, 26, 394–396 ; (b) H. Gilman, L. S. Miller, *J. Am. Chem. Soc.* 1951, 73, 2367–2368 ; (c) F. F. Brown, *J. Am. Chem. Soc.* 1965, 87, 4317–4324.

[30] (a) C. G. Armistead, A. J. Tyler, F. H. Hambleton, S. A. Mitchell, J. A. Hockey, *J. Phys. Chem.* 1969, 73, 3947–3953 ; (b) D. Derouet, S. Forgeard, J.-C. Brosse, J. Emery, J.-Y. Buzare, *J. Polym. Sci., Part A* 1998, 36, 437–453.

[31] (a) V. Bolis, A. Cavenago, A. B. Fubini, *Langmuir* 1997, 13, 895 ; (b) V. Bolis, B. Fubini, L. Marchese, G. Martra, D. J. Costa, *Chem. Soc., Faraday Trans.* 1991, 87, 497.

[32] (a) J. P. Blitz, R. S. S. Murphy, D. E. Leyden, *J. Am. Chem. Soc.* 1987, 109, 7141–7145 ;
(b) P. V. der Voort, E. F. Vansant, *Pol. J. Chem.* 1997, 71, 550–567 ; (c) X. S. Zhao, G. Q. Lu, *J. Phys. Chem. B* 1998, 102, 1556–1561.

[33] E. J. Cho, F. V. Bright, F. V. *Anal. Chem.* 2001, 73, 3289

[34] (a) L. Maron, L. Perrin, O. Eisenstein, *J. Chem. Soc., Dalton Trans.* 2002, 534 – 539 ; (b) Perrin, L. Maron, O. Eisenstein, *Inorg. Chem.* 2002, 41, 4355 – 4362.

[35] L. Maron, O. Eisenstein, *New J. Chem.* 2001, 255 – 258.

[36] G. Lapadula, A. Bourdolle, F. Allouche, M. P. Conley, I. del Rosal, L. Maron, W. W. Lukens, Y. Guyot, C. Andraud, S. Brasselet, C. Copéret, O. Maury, R. A. Andersen *Chem. Mater.*, 2014, *26*, 1062–1073

[37] (a) D. C. Bradley, Y. C. Gao *Polyhedron* 1982, 1, 307-310 ; (b) H. C. Aspinall, S. R . Moore, A. K. Smith *J. Chem. Soc. Dalton Trans.* 1992, 153 – 156.

[38] (a) J. P. Osegovic, R. S. Drago *Journal of Catalysis* 1999, 182, 1–4 ; (b) J. P. Osegovic, R. S. Drago *J. Phys. Chem. B* 2000, 104, 147-154